

MI-BASED IMAGE REGISTRATION USING
A NEW HISTOGRAM ESTIMATION SCHEME

Shaoyan Sun¹§, Liwei Zhang², Chonghui Guo³

^{1,2}Department of Applied Mathematics
Dalian University of Technology
Dalian, 116024, P.R. CHINA

¹e-mail: sunshaoyan1979@yahoo.com.cn

²e-mail: lwzhang@dlut.edu.cn

³Institute of System Engineering
Dalian University of Technology
Dalian, 116024, P.R. CHINA

e-mail: guochonghui@tsinghua.org.cn

Abstract: A new histogram estimation scheme is proposed in the calculation of mutual information (MI) for image registration. We show that the mutual information function derived from the new estimation scheme is continuous and differentiable, and we derive analytic expressions of its derivatives that allow numerically exact evaluation of its gradient. Both Powell and conjugate gradient methods are applied to optimize the MI function. Experimental results show that, compared with the MI using partial volume interpolation (PVI), the MI registration function derived from the suggested scheme reduces the interpolation-induced artifacts, encounters less local maxima and the registration performance is improved significantly.

AMS Subject Classification: 94A15, 94A08, 90C90

Key Words: image registration, mutual information, joint histogram estimation, Powell's method, conjugate gradient method

1. Introduction

Maximization of mutual information (MI) has been recently been proposed as a new approach for multimodal medical image registration [10, 1, 3] and has

Received: January 23, 2007

© 2007, Academic Publications Ltd.

§Correspondence author

been developed into an accurate measure for rigid image registration [5, 7]. The method applies the concept of mutual information (MI) to measure the statistical dependence between the image intensities of corresponding voxels in both images, which is assumed to be maximal if the images are geometrically aligned. Despite of the general promising results, MI-based matching can result in misregistrations in many cases because the registration function may be ill-defined, containing local maxima which will hamper the optimization process and influence the registration accuracy. Possible reasons for this are the artefacts induced by interpolation techniques or the absence of spatial information in the function [6, 9].

In this paper, a novel joint histogram estimation scheme has been designed in the calculation of MI to provide a more robust image registration. The MI function derived from the novel scheme is continuous and differentiable. We derive analytic expressions of its derivatives that allow numerically exact evaluation of its gradient. We investigate the performance of the MI measure based on the new histogram estimation approach (hereafter referred to as New-MI) and both Powell and conjugate gradient (CG) methods are employed to optimize our new MI function. Experimental results show that the proposed histogram scheme is feasible and leads to a better mutual information function.

2. Registration Process

In the discussion that follows, it is assumed that an “image” can have two or three dimensions.

2.1. The Mutual Information Criterion

Let f and r denote the image intensity values of a pair of corresponding voxels in the two images F (floating image) and R (reference image) that are to be registered. Then the MI registration criterion I of images F and R can be defined as follows:

$$I = \sum_{f,r} p_{fr} \log_2 \frac{p_{fr}}{p_f \cdot p_r}, \quad (1)$$

where p_{fr} , p_f and p_r represent the joint and marginal distributions of the pair (f, r) , f and r respectively. Intensities f and r are related through the geometric transformation T_α defined by the registration parameter α . The MI registration criterion states that the images are geometrically aligned by the transformation T_{α^*} for which I is maximal.

Generally, estimates for the distributions can be obtained by simple normalization of the joint and marginal histograms of the overlapping parts of both images. Consequently we can rewrite (1) as

$$I = \frac{1}{N} \sum_{f,r} h_{fr} \log_2 \frac{h_{fr}}{h_f \cdot h_r}. \quad (2)$$

Here h_{fr} , h_f and h_r are joint and marginal histograms respectively, where $h_f = \sum_r h_{fr}$, $h_r = \sum_f h_{fr}$ and $N = \sum_{f,r} h_{fr}$. To construct the joint histogram efficiently, the floating and the reference image intensities should be first linearly rescaled to the range $[0, n_F - 1]$ and $[0, n_R - 1]$, respectively, $n_F \times n_R$ being the total number of bins in the joint histogram [4]. Here, we use $n_F = n_R = 64$.

2.2. The Proposed Joint Histogram Estimation Scheme

Let Ω_F and Ω_R denote the discrete domains of the floating image F and the reference image R respectively. Let k be a voxel of image F at position p_k . The joint image intensity histogram $H = \{h_{fr}\}$ of the overlapping part of images F and R with image intensities $\{f\}$ and $\{r\}$ respectively is constructed by transforming samples $\{p_k\}$ in image F into samples $\{q_k = T_\alpha \cdot p_k\}$ in image R , and binning all pairs of corresponding voxel intensities $\{(f_k = F(p_k), r_k = R(q_k))\}$ for all $k \in \Omega_F$. The transformation T_α is restricted to rigid-body transformation in the current study, so for 3D image registration problem, the transformation parameter α is a six-component vector consisting of three rotation angles ϕ_x, ϕ_y, ϕ_z (measured in degrees) and three translation distances t_x, t_y, t_z (measured in millimeters).

In general, the position q_k will not coincide with a grid point of R , which will bring difficulty to the estimation of the joint histogram. Most researchers introduced interpolation techniques, such as nearest neighbor, bilinear and partial volume interpolation (PVI), to solve this problem. But as well known, existing interpolation methods can, in many cases, cause serious artefacts disrupting the registration function. In this paper, we design another method to construct the joint histogram. The reference image R is firstly partitioned into n_R iso-intensity sets, one for each set Ω_r with

$$\Omega_r = \{q \in \Omega_R | R(q) = r\}, \quad (3)$$

and then each entry h_{fr} in the histogram H is built up as the sum over all voxels k in the following manner:

$$h_{fr} = \sum_k \sum_{q \in \Omega_r \cap U(q_k, c)} e^{-(\|f - f_k\|^2 + \|q - q_k\|^2)}, \quad (4)$$

where $f_k = F(p_k)$, $q_k = T_\alpha \cdot p_k$ and $U(q_k, c)$ is a region of q_k in image R containing all the voxel positions q that satisfy the inequality $\|q - q_k\|_\infty < c$. It should be noted that by using $q \in U(q_k, c)$, all the voxels in the corresponding neighborhood region were also been considered during the computation of joint histogram. Experimentally the constant c was set to 2. Obviously, (4) is a continuous and differentiable function of the transformation parameter α , so the histogram and hence the MI are continuous as well as differentiable functions of α . These aforementioned characters can be expected to increase the smoothness of the New-MI registration function, and has the potential to improve the registration results. This can be validated in Section 3.

2.3. The Gradient of Mutual Information

It is easy to derive the analytic derivatives of our MI function according to expressions (2) and (4). Let α_ι denote the ι th component of vector α . If the derivatives $\partial H / \partial \alpha_\iota = \{\partial h_{fr} / \partial \alpha_\iota\}$ of the joint histogram w.r.t. the registration parameters α_ι exist, the gradient of mutual information can be written as

$$\nabla I(\alpha) = \left\{ \frac{\partial I}{\partial \alpha_\iota} \right\}, \quad (5)$$

$$\frac{\partial I}{\partial \alpha_\iota} = \frac{dI}{dh_{fr}} \cdot \frac{\partial h_{fr}}{\partial \alpha_\iota} = \frac{1}{N} \sum_{f,r} \left(\log_2 \frac{N \cdot h_{f,r}}{h_f \cdot h_r} - I \right) \frac{\partial h_{fr}}{\partial \alpha_\iota}. \quad (6)$$

Each gradient component ι is thus expressed as the sum over all histogram entries of the change in each entry when changing α_ι , weighed by the influence of this change on I .

From expression (4), it is easy to derive the analytic derivatives of H and the analytic expressions are as follows:

$$\begin{aligned} \frac{\partial h_{fr}}{\partial \alpha_\iota} &= \sum_k \sum_{q \in \Omega_r \cap U(q_k, c)} e^{-(\|f - f_k\|^2 + \|q - q_k\|^2)} \cdot \left[-2 \langle q - q_k, \frac{\partial(-q_k)}{\partial \alpha_\iota} \rangle \right] \\ &= 2 \sum_k \sum_{q \in \Omega_r \cap U(q_k, c)} e^{-(\|f - f_k\|^2 + \|q - q_k\|^2)} \cdot (q - q_k)^T \cdot \frac{\partial q_k}{\partial \alpha_\iota} \\ &= 2 \sum_k \sum_{q \in \Omega_r \cap U(q_k, c)} e^{-(\|f - f_k\|^2 + \|q - q_k\|^2)} \cdot (q - q_k)^T \cdot \frac{\partial T_\alpha}{\partial \alpha_\iota} \cdot p_k. \quad (7) \end{aligned}$$

Expressions for $\partial T_\alpha / \partial \alpha_\iota$ can be computed straightforward for each of the translation and rotation parameters.

2.4. Optimization

Powell’s method is a reasonable method between robustness and speed, and requires no gradient evaluations. It is used to optimize the two different registration functions, the convergence parameters for the Brent’s line maximization and Powell’s optimization algorithm are set to 10^{-3} and 10^{-4} respectively, see [8].

In addition, we also apply conjugate gradient (CG) method to optimize the mutual information function derived from the suggested histogram estimation scheme since it is differentiable, see [8]. The convergence parameters for the Brent’s line maximization and CG optimization algorithm are also set to 10^{-3} and 10^{-4} respectively.

3. Experiments and Results

3.1. Registration Functions

To visually evaluate the performance of our New-MI, we first plot the registration functions with respect to translations in both x and y directions. T1 and T2 MRI 2D image slices from the *Brain Web Simulated Brain Database* (see [2]) of size 181×217 are used to produce the landscape, and the MI function based on PV interpolation (hereafter referred to as PVI-MI) has also been considered for comparison. T2 MRI was taken as the floating image. It should be noted that the image pair have already been perfectly aligned.

Figure 1 contains the registration functions for translations in both x and y directions using the PVI-MI respectively. The top row shows the functions using the whole original data, while in the bottom row the functions are given after the floating image has been equidistantly subsampled by a factor of three in each dimension. Clearly, all the PVI-MI functions have maxima at grid positions, especially when the floating image has been subsampled. It is obvious that optimization of such functions will not be robust and accurate. By using the new histogram estimation method, the New-MI functions are vastly improved which are less sensitive to low sampling resolution and local maxima are nearly eliminated. These can be expected to increase the registration performance of the MI function.

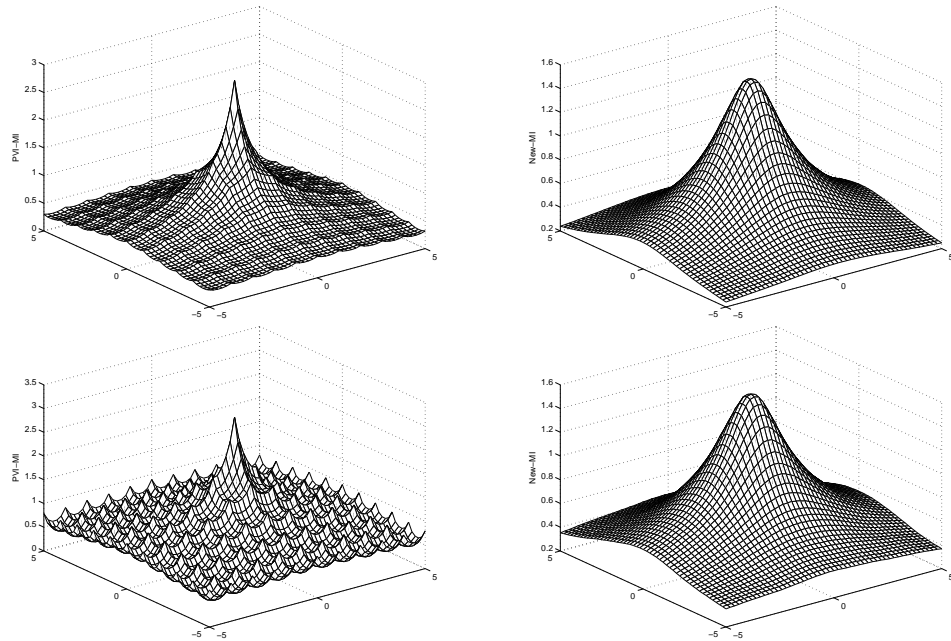


Figure 1: Registration functions with respect to translations in both x and y directions (in millimeters). From top to bottom: (i) original data, (ii) subsampled data.

Data	Results ($[t_x, t_y, \phi_x]$)	Function evaluations
Original data	$[-0.0450, -0.0163, -0.1290] \times 10^{-3}$	201
Subsampled data	$[11.9454, -4.8590, 14.9733]$	154 (failed)

Table 1: PVI-MI measure optimized by Powell's method

3.2. Simulated 2D Registration Results

Further simulated registration experiments are carried out to evaluate our proposed method on the aforementioned 2D data. Prior to starting the optimization process, the floating image was transformed with an initial registration parameter $\alpha_0 = [t_x, t_y, \phi_x] = [10, -5, 15]$. Complete registration is obtained when $\alpha = [0, 0, 0]$.

The results we obtained using PVI-MI and New-MI are listed respectively in Table 1, Table 2 and Table 3. From Table 1 it is clear that the performance of the PVI-MI function is vastly decreased when the floating image was sub-

Data	Results $([t_x, t_y, \phi_x])$	Function evaluations
Original data	$[-0.0011, -0.0009, 0.0011]$	161
Subsampled data	$[-0.0020, 0.0027, 0.0045]$	218

Table 2: New-MI measure optimized by Powell’s method

Data	Results $([t_x, t_y, \phi_x])$	Function evaluations	Gradient evaluations
Original data	$[-0.8453, -0.4514, -0.8583] \times 10^{-3}$	208	126
Subsampled data	$[-0.3111, -0.0635, -0.3866] \times 10^{-3}$	115	77

Table 3: New-MI measure optimized by conjugate gradient method

sampled by a factor of three, the function gets into a local maximum and results in a misregistration; while for the proposed method, the sub-sampling operation almost does not affect its performance and it yields satisfactory results in all cases. The new measure optimized by CG optimization provides the best overall behavior.

3.3. Clinical 3D Registration Results

Registration of PET and MR images is a considerably more difficult problem, both because of the fewer similarities between the image contents and because of the lower intrinsic resolution of PET images. Here, we evaluate the New-MI registration measure for matching of two clinical 3D images: image PET ($128 \times 128 \times 15$ voxels, $2.59 \times 2.59 \times 8$ mm) and image MR_PD ($256 \times 256 \times 26$ voxels, $1.25 \times 1.25 \times 4$ mm). These two images were furnished by Vanderbilt University as the practice data set, for which the reference registration solutions were available to us [11].

We started all the registration tasks at zero vector. The difference between the reference and each of the MI registration solutions was evaluated at eight points near the brain surface. The registration error of our computational results was computed as follows:

$$error = \frac{1}{8} \sum_{i=1}^8 \|q_{i,reference} - q_i\|_2, \quad (8)$$

where $q_{i,reference}$ represents the i_{th} point’s coordinate provided by Vanderbilt University, and q_i is the coordinate we computed. The results are summarized

Registration criterion	Optimization method	Registration error (measured in mm)	Function evaluations	Gradient evaluations
PVI-MI	Powell	7.8625	755	None
New-MI	Powell	7.7446	506	None
New-MI	CG	6.7588	262	85

Table 4: Registration errors for PET/PD using different methods

in Table 4. All the registration errors were thus < 1 PET voxel (8 mm), and the result obtained by optimizing our New-MI measure using CG is the best, which is consist of the conclusion drawn from the simulated 2D registration results.

4. Conclusions

As mutual information is based on estimating probability distributions, the registration function is generally less smooth when the number of samples is small, for example, for low resolution images or in multi-resolution methods. In the present paper, a new histogram estimation scheme is proposed to provide a continuous and differentiable MI function. Experimental results indicate that compared with PVI-MI, the New-MI measure derived from the proposed histogram estimation scheme contains fewer erroneous maxima and improves the registration performance significantly.

Acknowledgments

This research is supported by Natural Science Foundation of China (Grant No. 10571018). The clinical images and their standard transformations were provided as part of the project, “Retrospective Image Registration Evaluation”, National Institutes of Health, Project Number 1 R01 NS33926-01, Principal Investigator Professor J. Michael Fitzpatrick, Vanderbilt University, Nashville, TN.

References

- [1] A. Collignon, F. Maes, D. Delaere, D. Vandermeulen, P. Suetens, G. Machal, Automated multi-modality image registration based on information theory, *IPMI – Information Processing in Medical Imaging* (1995), 263-274.

- [2] D.L. Collins, A.P. Zijdenbos, V. Kollokian, J.G. Sled, N.J. Kabani, C.J. Holmes, A.C. Evans, Design and construction of a realistic digital brain phantom, *IEEE Trans. Med. Imaging.*, **17** (1998), 463-468.
- [3] F. Maes, A. Collignon, D. Vandermeulen, G. Marchal, P. Suetens, Multimodality image registration by maximization of mutual information, *IEEE Trans. Med. Imaging.*, **6** (1997), 187-198.
- [4] F. Maes, D. Vandermeulen, P. Suetens, Comparative evaluation of multiresolution optimization strategies for multimodality image registration by maximization of mutual information, *Med. Image. Anal.*, **3** (1999), 373-386.
- [5] J.B.A. Maintz, M.A. Viergever, A survey of medical image registration, *Med. Image. Anal.*, **2** (1998), 1-36.
- [6] J.P.W. Pluim, J.B. A. Maintz, M.A. Viergever, Image registration by maximization of combined mutual information and gradient information, *IEEE Trans. Med. Imaging.*, **19** (2000), 1-6.
- [7] J.P.W. Pluim, J.B. A. Maintz, M.A. Viergever, Mutual-information-based registration of medical images: a survey, *IEEE Trans. Med. Imaging.*, **22** (2003), 986-1004.
- [8] W.H. Press, B.P. Flannery, S.A. Teukolsky, W.T. Vetterling, *Numerical Recipes in C*, Cambridge Univ. Press., Cambridge (1992).
- [9] D. Rueckert, M.J. Clarkson, D.L.G. Hill, D.J. Hawkes, Non-rigid registration using higher-order mutual information, In: *Proceedings of SPIE, Medical Imaging: Image Processing*, **3979** (2000), 438-447.
- [10] P. Viola, W.M. Wells III, Alignment by maximization of mutual information, In: *Proc. 5-th Int. Conf. Computer Vision*, **5** (1995), 16-23.

- [11] Vanderbilt Univ., T.N. Nashville, *Retrospective Image Registration Evaluation (RIRE)*, Available online at: [http://www. Vuse. Vanderbilt. Edu/ image/registration/](http://www.Vuse.Vanderbilt.Edu/image/registration/)